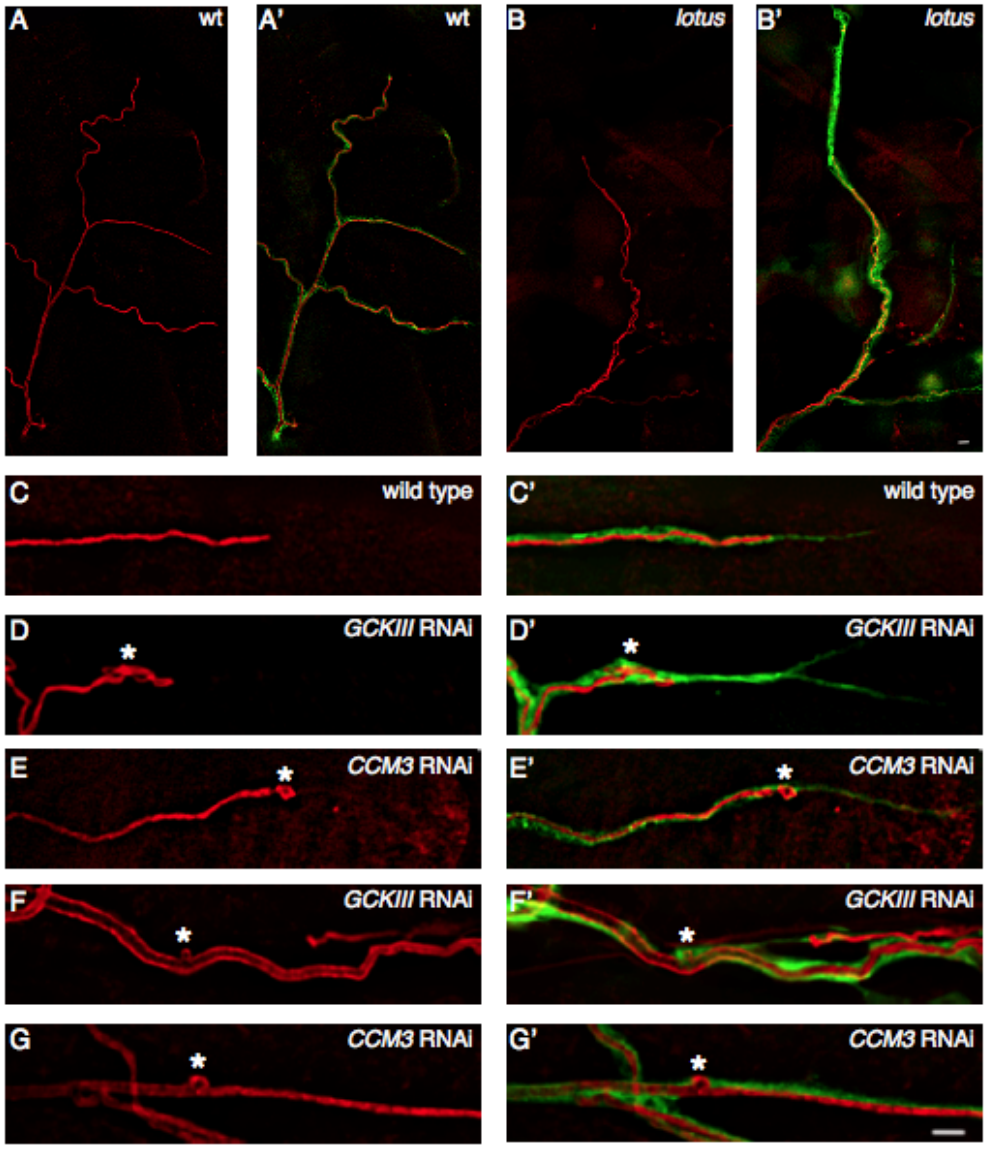

Figure S1; associated with Figure 1. Terminal cells mutant for *lotus* or *wheezy* or

knocked-down for *CCM3* display subtle tube defects outside the terminal zone. In mosaic animals, positively marked terminal clones are marked with GFP (green) and seamless tubes are visualized with α-Wkdpep staining (red). (A, A') Control wild type terminal cells extend branches in which single seamless tubes can be detected. In (B,B') lotus mutant terminal cells, we often detect two or more seamless tubes piercing a single cytoplasmic extension. This phenotype is reminiscent of the branch retraction defect observed for mutations affecting integrin-based adhesions (Levi et al., 2006). When examining the blind-ended tubes at the tips of terminal cells (wild type control; C, C'), we found that *GCKIII* RNAi (D, D') and *CCM3* RNAi (E, E') cells frequently displayed disorganized lumenal membrane. Additionally, we detected small microdilations at scattered positions throughout terminal cells in which GCKIII (F, F') or CCM3 (G, G') had been knocked down. In D – G', the asterisk marks the seamless tube defect. All larvae were third instar. Scale bars = 5 microns.

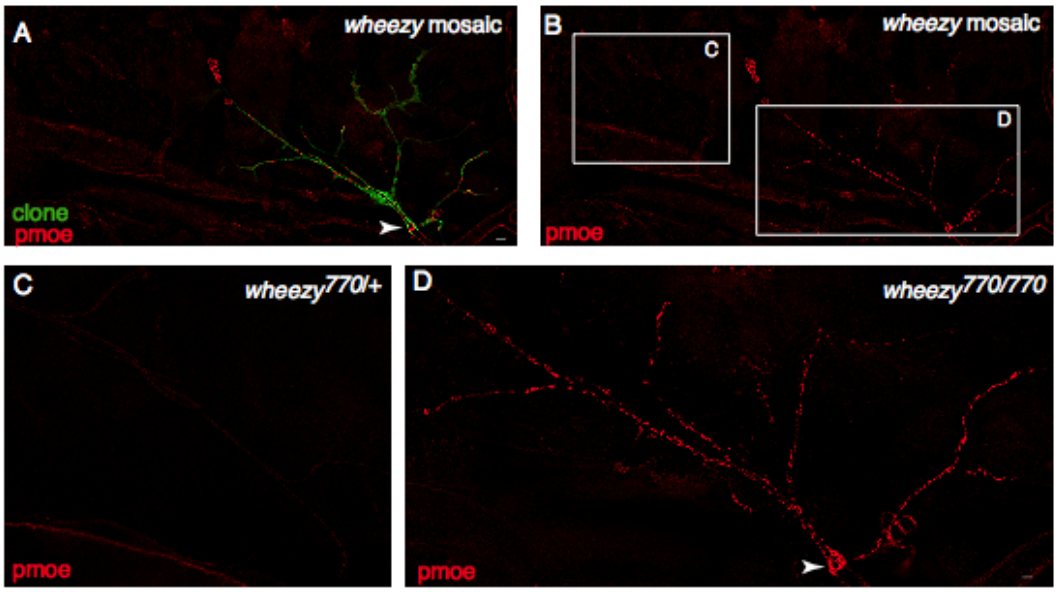

Figure S2; associated with Figure 3. Levels of phospho-Moesin are elevated in

***wheezy* clones.** Genetic mosaic third instar larvae were fixed and filleted and stained using an α-phospho-Moesin antibody. In (A), a homozygous mutant terminal cell is positively labeled with GFP (clone, green), and phosphorylated Moesin in the entire fillet is stained (pmoe, red). In (B), only phospho-Moesin staining is shown. A heterozygous terminal cell and a homozygous *wheezy* terminal cell are indicated by white rectangles, and are shown enlarged in (C) and (D), respectively. Striking enrichment of p-Moe around the transition zone tube dilation is indicated by arrowhead. Scale bars = 5 microns.

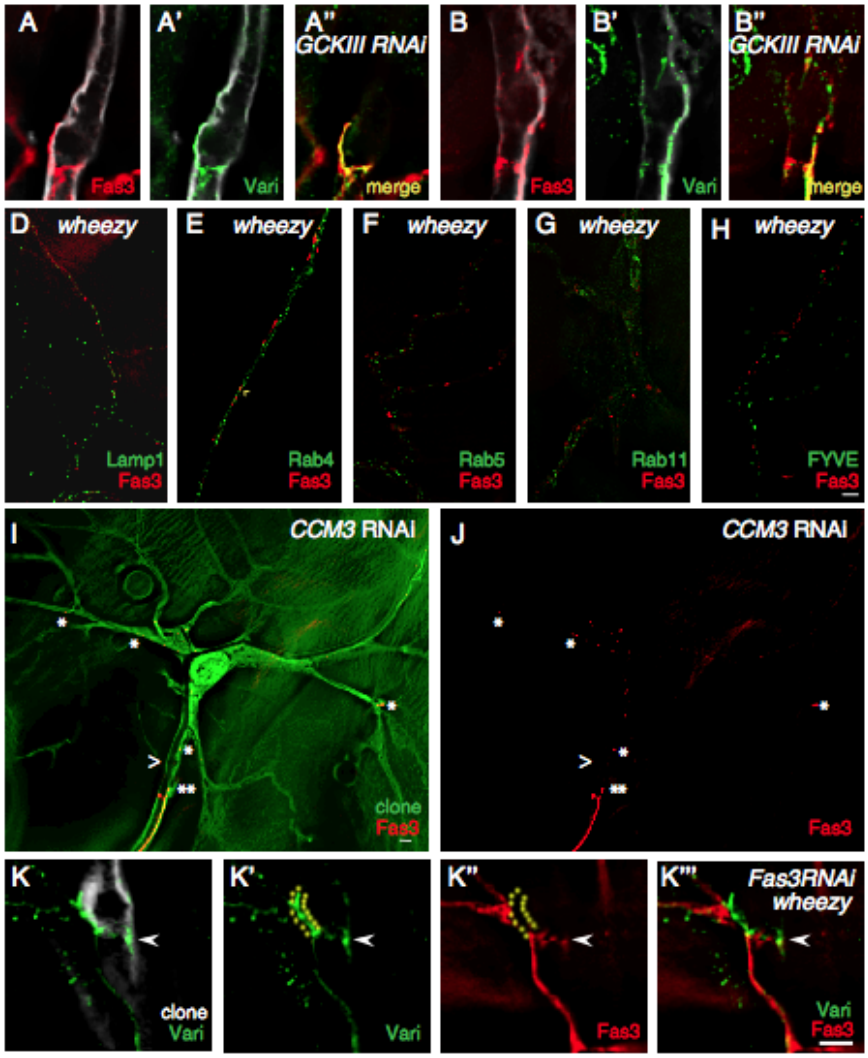

Figure S3; associated with Figure 4. CCM3/GCKIII deficient terminal cells showed

perdurance of septate junctions in the transition zone and mislocalized septate junction proteins. In A-B’’’, co-staining of Fas3 (A, A’’, B, B’’, red) and Varicose (A’, A’’, B’, B’’, green) in animals with pan-tracheal *GCKIII* knock-down (all tracheal cells are marked with GFP, A, A’, B, B’, white) suggest that functional septate junctions extend into the transition zone. To test whether ectopic patches of Fas3 in *wheezy* mutant terminal cells were transiting endocytic compartments, co-staining was carried out between Fas3 (D, E, F, G, H; red) and a series of markers: GFP-Lamp1 fusion protein (D, green), or YFP-Rab4 (E, green), YFP-Rab5 (F, green), Rab11, (G, green) or a GFP-FYVE fusion protein (H, green). Little co-staining (E, yellow arrowhead) was observed. Pan-tracheal knockdown of CCM3 (I,J) resulted in transition zone dilation (marked by > in I) and ectopic Fas3 staining. In (J), Fas3 staining is featured. The double asterisk marks a line of septate junction staining extending into the transition zone while select patches of ectopic Fas3 staining in the terminal cell are marked with single asterisks. In (K-K’’’), we tested whether the septate junctions present in the terminal cell transition zone were generated by the terminal cell, or belonged to the neighboring cell (the finger in a balloon model of Uv et al., 2003). For this experiment, we generated MARCM clones that were homozygous mutant for wheezy and also knocked-down for Fas3 (note: Fas3 knock-down occurs exclusively in the homozygous mutant cells, which were positively marked with GFP (white, K). In the mutant cell depicted, we detected septate junction in the transition zone (transition zone septate junction has been indicated by outlining with yellow dots in K’ and K’’) as marked by Varicose staining (K, K’, and K’’’, green). Fas3 staining (K’’, K’’’, red) was absent from the transition zone septate junction (K’’, not absence of Fas3 within region outlined by yellow dots), but clearly

detected in the neighboring stalk cell (K’’). This definitively shows that the septate junction, and its associated tube within the terminal cell, are generated by the terminal cell and not its neighbor – terminal cell is above the intercellular junction (indicated by arrowhead) and the stalk cell is below it. Larvae were at third instar. Scale bar = 5 microns

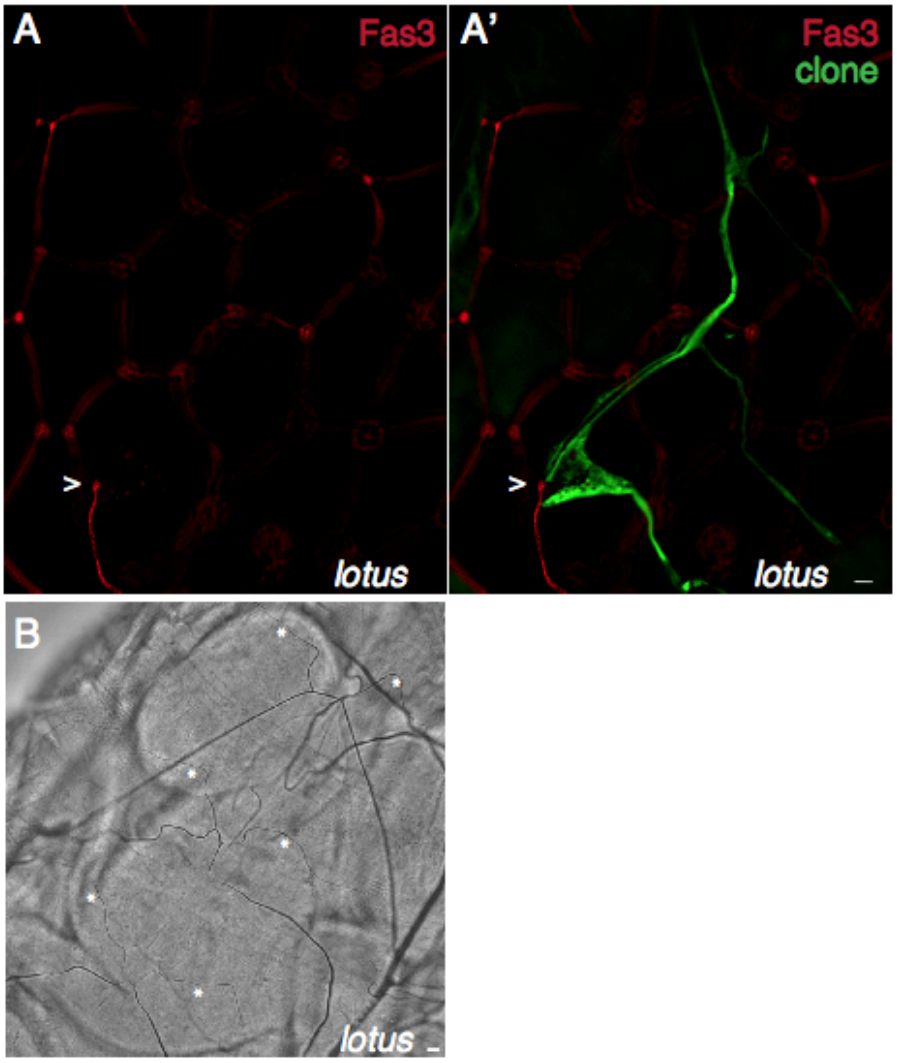

Figure S4; associated with Figure 2. In *lotus* mutants septate junctions appear

normal, and transition zone defects arise late. Mosaic third instar larvae were fixed and filleted and stained for GFP (green) to mark homozygous mutant *lotus* cells, and for Fas3 (red) to stain septate junctions. In (A), the seam of the neighboring heterozygous auto-cellular stalk cell can be seen terminating in a ring (indicated by >) that marks the intercellular junction with the *lotus* mutant tip cell (merge of Fas3 and clone marker in A'). Septate junctions between hexagonal-shaped epidermal cells are visible, slightly out of focus, in the background. No projection of septate junctions into the terminal cell can be detected. In (B), a homozygous *lotus* mutant first instar larva is shown by brightfield microscopy; no tube or gas-filling defects can be detected at this stage. Terminal cells are indicated by *. Scale = 5 microns.

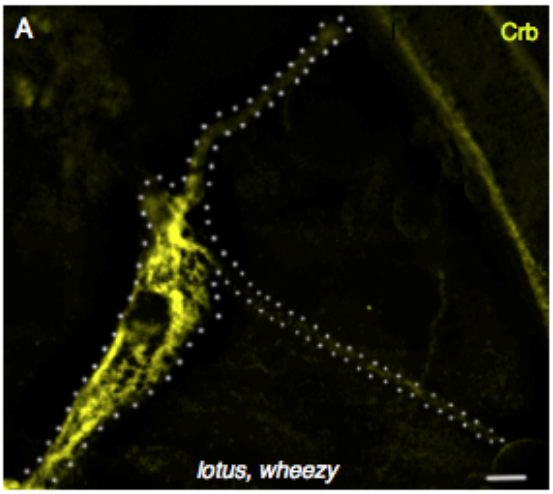

Figure S5; associated with Figure 5. Analysis of *lotus*, *wheezy* double mutant

terminal cells. In *lotus, wheezy* double mutant terminal cells (terminal cell outlined with white dots), Crumbs (yellow) levels appeared elevated but not restricted to the lumenal membrane. Larva was at third instar. Scale bar = 5 microns.

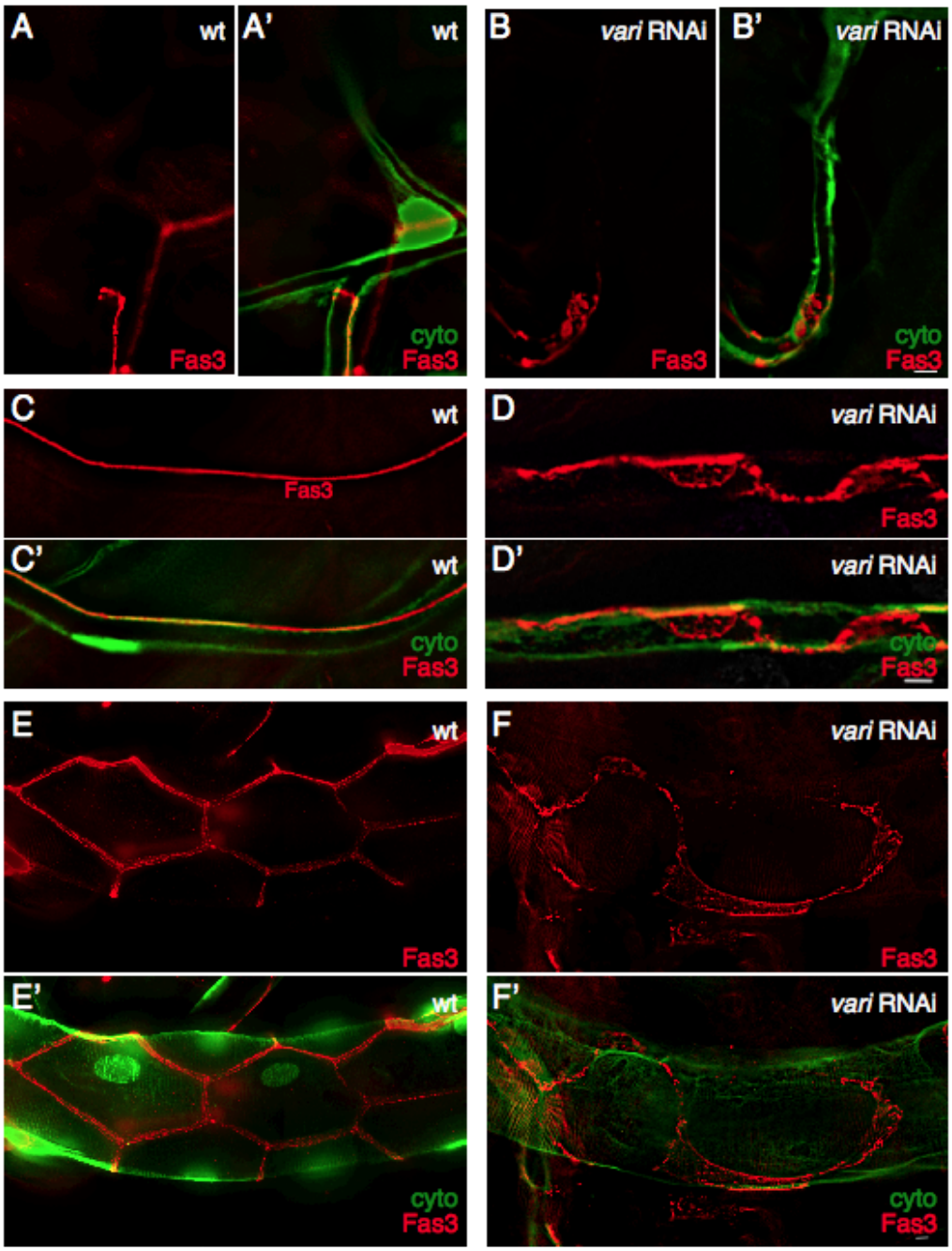

Figure S6; associated with Figure 6. Knockdown of *varicose* broadens and disrupts

septate junction staining. In animals subjected to knock-down of *varicose* at 25 ^{o}C we observed disruption of septate junctions. Compared to wild type controls (A, C, E), RNAi expressing animals showed less well defined septate junctions – Fas3 staining (red) was spread over a wider area and was not continuous. Terminal cells (A,B), stalk cells (C,D) and dorsal trunk cells (E,F) with seamless, auto-cellular and multi-cellular tubes, respectively, are shown. Cyto = cytoplasm as labeled by GFP. Larvae were third instar. Scale bars = 5 microns.

Supplemental Tables

RNAi construct expressed (VDRC stock #)	GAL4 driver and Copy Number	Phenotypes scored (% observed)			Terminal cells scored
		Transition Zone Tube Dilation	Terminal cell Gas-filling defect	Lumenized Terminal Cells	
none	2x btl-GAL4	0%	2%	100%	44
	1x btl-GAL4	0%	7%	100%	46
GCKIII RNAi (107158)	2x btl-GAL4	69%	6%	100%	51
	1x btl-GAL4	37%	7%	100%	46
GCKIII RNAi (49559)	2x btl-GAL4	16%	2%	N/D	48
	1x btl-GAL4	**0%**	**2%**	**N/D**	49
GCKIII RNAi (49558)	2x btl-GAL4	8%	4%	100%	49
	1x btl-GAL4	9%	4%	100%	46
CCM3 RNAi (46548)	2x btl-GAL4	23%	0%	100%	48
	1x btl-GAL4	4%	0%	100%	51
CCM3 RNAi (106841)	2x btl-GAL4	lethal	lethal	lethal	-
	1x btl-GAL4	**7%**	**17%**	**100%**	42
	1x srf-GAL4	8%	10%	100%	49
CCM3 RNAi (109453)	2x btl-GAL4	lethal	lethal	lethal	-
	1x btl-GAL4	2%	33%	100%	46

Table S1; Associated with Figures 3 and 4: Quantification of *GCKIII* and *CCM3* RNAi phenotypes. Tracheal-specific GAL4 driver lines (*btl*, pan-tracheal; *srf*, terminal cell specific) were crossed to RNAi strains targeting either *GCKIII* or *CCM3* for knock-down. Control animals were from a cross to yw^{1118} flies. Progeny from all crosses also carried a UAS-GFP transgene to allow fluorescent imaging of tracheal cells. Terminal cells from third instar larvae were assayed for tube dilation in the transition zone, gas-filling, and tube formation ("lumenized terminal cells"). Crosses equivalent to those reported by Chan and colleagues, and using the same RNAi strains, are indicated by bold lettering. N/D = not done.

Genotype	Mean # of microdilations/length of lumen (mm) +/- S.E.M.	Terminal cells scored
wheezy	101±62	10
$vari^{RNAi}$*; wheezy*	93±106	10

Table S2; Associated with Figure 6: Quantification of small bulges.

The number of small bulges was determined in terminal cells mutant for *wheezy* or mutant for *wheezy* and knocked-down for *varicose*. Clones were identified by GFP expression and bulges were scored by α-Wkdpep staining. The difference in the number of bulges observed between the two genotypes was not significant ($P>0.05$).

Supplemental Movies

Movie S1; Associated with Figure 6: 3-D projection of *lotus, wheezy* terminal cell clone. In this movie, a 3-D projection of a deconvolved Z-stack through a *lotus, wheezy*

double mutant terminal cell from a third instar larva is shown. The clone was positively marked with GFP (green) and its lumen visualized with α-Wkdpep staining (red). A continuous transition zone tube without dilation can be seen.